PERGAMON

Deep-Sea Research I 49 (2002) 1725–1739

DEEP-SEA RESEARCH
PART I

www.elsevier.com/locate/dsr

New production of the NW Iberian shelf during the upwelling season over the period 1982–1999

X.A. Álvarez-Salgado[a,*], S. Beloso[a], I. Joint[b], E. Nogueira[a], L. Chou[c], F.F. Pérez[a], S. Groom[b], J.M. Cabanas[d], A.P. Rees[b], M. Elskens[e]

[a] *CSIC, Instituto de Investigacións Mariñas, Eduardo Cabello 6, 36208-Vigo, Spain*
[b] *Plymouth Marine Laboratory, Prospect Place, The Hoe, Plymouth PL1 3DH, UK*
[c] *Laboratoire d'Océanographie Chimique et Géochimie des Eaux, Université Libre de Bruxelles, Campus de la Plaine—CP 208, B-1050 Brussels, Belgium*
[d] *Centro Oceanográfico de Vigo, Instituto Español de Oceanografía, Cabo Estay, 36200-Vigo, Spain*
[e] *Laboratory of Analytical Chemistry, Vrije Universiteit Brussel, Pleinlaan 2, B-1050 Brussels, Belgium*

Received 26 February 2001; received in revised form 13 February 2002; accepted 27 June 2002

Abstract

New production (NP) is calculated for NW Iberian shelf waters from 42° to 43°N (3500 km^2), at the fortnight, upwelling-season (March–October) and inter-annual time-scales. The time series used are (1) upwelling rates (daily values of offshore Ekman transport from 1982 to 1999), (2) bottom shelf temperatures (twice a week values from 1987 to 1999), and (3) the nutrient–temperature relationships of upwelled Eastern North Atlantic Central Water (ENACW) obtained during 14 hydrographic cruises to the study area (between 1977 and 1998). Marked inter-annual variability is observed, both at the fortnight and the seasonal time-scales. Average NP over the upwelling-season ranged from 330 to 815 mg C m^{-2} d^{-1} (mean, 490 ± 145 mg C m^{-2} d^{-1}) in the 1982–1999 period. Large inter-annual changes of upwelling rates are the reason behind the NP fluctuations: 83% of the variability of NP can be explained by the offshore Ekman Transport ($-Q_X$). NP is compared with satellite-derived net microbial community production (NCP) during the 1998–1999 upwelling seasons, when SeaWiFS images are available. An average upwelling-season NP/NCP ratio of 0.33 was obtained, indicating that 67% of NCP is respired in situ and 33% is exported off-shelf to the surrounding oligotrophic ocean.

Keywords: Upwelling; Nutrients; New production; NW Iberian margin

1. Introduction

The concept of new production (NP) is one of the cornerstones of marine ecology, since it constrains both the sustainable exploitation of marine resources and the role of the oceans in the regulation of excess anthropogenic CO_2 accumulation in the atmosphere. NP is simply defined as the

*Corresponding author. Tel.: +34-986-231-930; fax: +34-986-29-27-62.
E-mail address: xsalgado@iim.csic.es (X.A. Álvarez-Salgado).

0967-0637/02/$ - see front matter
PII: S0967-0637(02)00094-8

fraction of the gross primary production (GPP) that is maintained by external nutrients, and the NP/GPP quotient is traditionally called '*f*-ratio' (Eppley and Peterson, 1979; Kauner, 1993). The spatial scales (from local to global) and the time scales (days to thousands of years) of the study area define what should be considered as 'external' to the system. The NP may be either (1) accumulated in the system (hence increasing internal resources), (2) transferred to higher trophic levels, or (3) exported both vertically and laterally out of the region of study. When sufficiently long space and time scales are considered, say when 2–3 times the flushing rate of the study ecosystem is considered, steady-state conditions can be assumed; in this case, transference to higher trophic levels can be neglected, NP is equal to the export production of the system. NP can be exported either vertically (to deep waters in the open ocean or the sediments in the coastal zone) or horizontally (to surrounding ecosystems). In terms of marine resources, the *f*-ratio represents the fraction of the GPP that can be exploited without affecting the long-term integrity and stability of the ecosystem (Quiñones and Platt, 1991). In relation to global change, $1/f$-ratio represents the number of times that a carbon atom cycles between CO_2 and organic matter before leaving the system (Middleburg et al., 1993). The lower the *f*-ratio the higher the time of contact of the CO_2 molecules with the atmosphere and, therefore, the lower the efficiency of the system as a CO_2 sink.

Although the concept of *f*-ratio is simple, its estimation can be rather complicated and has been controversial. Calculation of the flux of external nutrients, specifically the limiting nutrient, should be the most direct way to evaluate NP, but it requires detailed knowledge of the chemical characteristics and the fluxes of all relevant atmospheric, continental and ocean sources. In addition, GPP rates compatible with the space and time scales of the NP estimate should be determined too. For spatial scales $>10^3\,km^2$ satellite-derived estimates are likely the most convenient method to appraise primary production rates. Carbon uptake measurements and a mathematical model that quantitatively relate primary production to satellite-based estimates of chlorophyll concentration have to be combined to obtain satellite-derived primary production rates (Behrenfeld and Falkowski, 1997). The ^{14}C method is commonly used to measure carbon uptake by marine phytoplankton; the incubation time states whether the ^{14}C measurements represent either gross (GPP) or net microbial (NCP) community production (Laws, 1991; Williams, 1993). The difference between GPP and NCP is due to the respiration (R) of phytoplankton and the heterotrophs collected in the incubation bottles (mainly microzooplankton and bacteria). The oxygen light and dark bottle method provides an independent determination of NCP and R (Strickland and Parsons, 1972). Comparison of these NP and GPP estimates at comparable space and time scales allow determination of an ecosystem-level *f*-ratio, i.e. an *f*-ratio that accounts for the metabolic requirements of the whole community of organisms in the ecosystem.

As an alternative to this ecosystem-level method, Eppley and Peterson (1979) proposed a microbial method based on the incorporation of $^{15}NH_4^+$ and $^{15}NO_3^-$ by the microbial communities of the study system assuming that all, and only, the NO_3^- is external to the system. This operational definition has been subsequently modified to include the contribution of urea to the total nitrogen uptake, hence reducing considerably the original *f*-ratios (Wafar et al., 1995). However, the method has shortcomings in coastal studies, where not all the external nitrogen has to be in the NO_3^- form and nitrification may be a NO_3^- source within the boundaries of the system (Wollast, 1993). Comparison of NCP and R measurements obtained with the light and dark oxygen incubation method can also be used to obtain an *f*-ratio $=NPP/(NCP+R)$ that accounts for the metabolic requirements of the microbial communities (Quiñones and Platt, 1991).

Coastal upwelling areas are particularly important in the context of the exploitation of resources and of the air–sea exchange of anthropogenic CO_2, and knowledge of the magnitude of NP of these areas is of great importance. Although approximate global estimates are available (e.g. Walsh, 1991; Wollast, 1993, 1998), detailed studies incorporating different time scales of variability are

scarce. This is especially true for the NW Iberian margin. Coastal winds off NW Spain describe a conspicuous seasonal cycle, favouring upwelling from March–April to September–October and downwelling for the rest of the year (Wooster et al., 1976; Bakun and Nelson, 1991). The water that is upwelled to the surface originates from either subpolar (temperature $<13^{\circ}C$) or subtropical (temperature $>13^{\circ}C$) branches of Eastern North Atlantic Central Water (ENACW; Fiúza, 1984; Ríos et al., 1992). Upwelling/relaxation cycles as a result of coastal winds occur with a periodicity of $\sim$10–20 days during the upwelling season (Blanton et al., 1987; Álvarez-Salgado et al., 1993), hence modulating the entry, and allowing the complete consumption, of new nutrients within the surface mixed layer (Álvarez-Salgado et al., 2001).

The objective of this work is to assess the NP of the NW Iberian shelf (42–43°N) during the upwelling-favourable season. The approach combines the thermohaline and chemical (nitrate, phosphate and silicate) characteristics of ENACW with upwelling rates derived from computations of Ekman transport. Bi-weekly, seasonal and interannual variabilities are examined. NP is compared with satellite-derived NCP for the NW Iberian upwelling.

2. Material and methods

2.1. Nutrient–temperature relationships in upwelled waters off NW Spain

Nutrient–temperature relationships of upwelled ENACW were determined for 14 cruises in the NW Iberian upwelling system, from 1977 to 1998 (Table 1). Nutrient concentrations of nitrate, phosphate and silicate were analysed by standard colorimetry, using either automatic segmented flow analysis or manual methods.

The analysis considers only stations with water depth >1000 m (Fig. 1) to avoid the well-described nutrient enrichment in shelf bottom waters by intense mineralisation (Álvarez-Salgado et al., 1993, 1997). Data from a total of 128 casts were analysed in the area between latitudes 42° and 43°N, and between 11°W and the 1000 m depth isobath. ENACW off NW Spain has traditionally been considered to be between the salinity maximum of the warmest subtropical ENACW branch at 50–100 m depth and the salinity minimum of the coldest subpolar ENACW branch at 450–500 m depth (Ríos et al., 1992; Pérez et al., 1993). Following this criterion, a total of 706 ENACW samples were selected from the 128 casts, i.e. an average of 5–6 samples per cast.

Table 1
Relevant information about the cruises used in this work, including sampling dates, vessel and sampling gear

Cruise	Dates	Research vessel	Sampling gear
GALICIA–IV	7–28 Oct 1977	Cornide de Saavedra	Niskin bottles with inv. therm.
GALICIA–V	9–20 Nov 1982	García del Cid	Niskin bottles with inv. therm.
GALICIA–VI	1–12 Dec 1983	García del Cid	Niskin bottles with inv. therm.
GALICIA–VII	18 Feb–7 Mar 1984	García del Cid	Niskin bottles with inv. therm.
GALICIA–VIII	13–24 Jul 1984	García del Cid	Niskin bottles with inv. therm.
GALICIA–IX	3 Sep–4 Oct 1986	García del Cid	Niskin bottles with inv. therm.
GALICIA–XI	5–10 May 1991	Investigador S.	CTD, rosette sampler
GALICIA–XII	10–18 Sep 1991	Investigador S.	CTD, rosette sampler
MORENA–I	10–26 May 1993	Cornide de Saavedra	CTD, rosette sampler
CD105	12–20 Jun 1997	Charles Darwin	CTD, rosette sampler
Bg9714	19–29 Jun 1997	Belgica	CTD, rosette sampler
CD110b	6–16 Jan 1998	Charles Darwin	CTD, rosette sampler
CD114	1–20 Aug 1998	Charles Darwin	CTD, rosette sampler
Bg9815c	26 Jun–7 Jul 1998	Belgica	CTD, rosette sampler

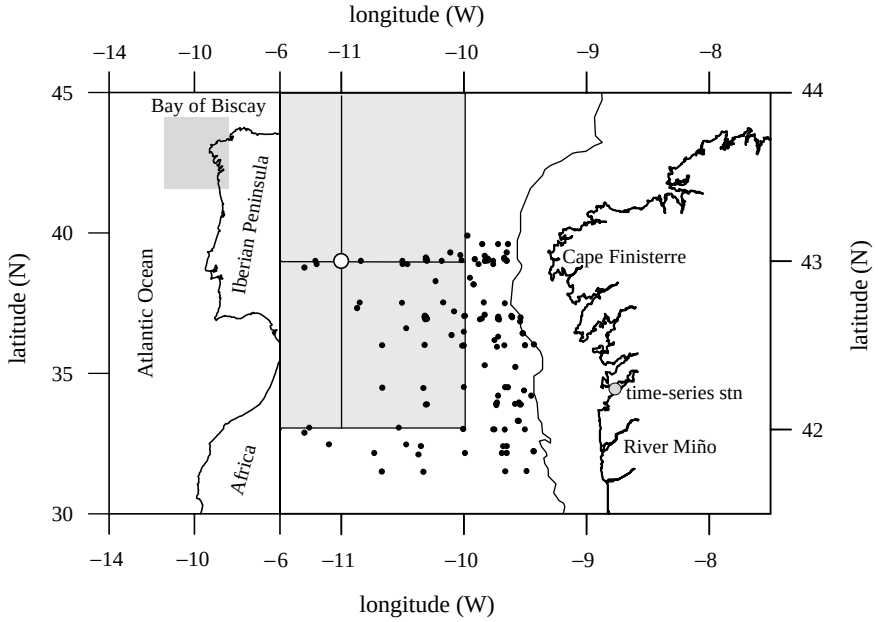

Fig. 1. Chart of the study area, the NW Iberian upwelling system at 42–43°N. Black circles, position of the 128 selected sampling stations during the 14 study cruises (Table 1). The open circle is the centre of the $2^\circ \times 2^\circ$ geostrophic cell (shaded area in the right panel) at 43°N 11°W. The grey circle is the position of the time-series station of the 'Ría de Vigo'. Solid line, 1000-m bathymetric contour.

2.2. Time series of offshore Ekman transport at 43°N 11°W

The northerly component of shelf wind-stress (τ_y) causes upwelling-favourable offshore Ekman transport ($-Q_X$) along the western Iberian margin (Wooster et al., 1976), and southerly winds result in the opposite effect, i.e. downwelling and onshore transport. Ekman transport can be approximately estimated by Bakun's (1973) method

$$-Q_X = \frac{\tau_y}{\rho_W f} = -\frac{\rho_{air} C_D |V| V_y}{\rho_W f}, \quad (1)$$

where ρ_{air} is the density of air ($1.22\,kg\,m^{-3}$ at 15°C), C_D is an empirical dimensionless drag coefficient (1.4×10^{-3} according to Hidy, 1972), f is the Coriolis parameter ($9.946 \times 10^{-5}\,s^{-1}$ at 43° latitude), ρ_{SW} is the density of seawater ($\sim 1025\,kg\,m^{-3}$), and $|V|$ and V_y are the average daily module and northerly component of the geostrophic winds in a $2^\circ \times 2^\circ$ cell centred at 43°N 11°W, representative for the study area (shaded area in the right panel of Fig. 1). Average daily geostrophic winds were estimated from atmospheric surface pressure charts, provided at 6-h intervals by the 'Instituto Nacional de Meteorología'. Positive values of $-Q_X$ ($m^3\,s^{-1}\,km^{-1}$) indicate upwelling-favourable offshore Ekman transport. Conversely, negative values of $-Q_X$ indicate downwelling-favourable onshore Ekman transport (see Lavín et al., 1991 for further details).

A time series of daily values of $-Q_X$ from January 1982 to December 1999 ($n = 6574$) was analysed. Values outside the lower extreme boundary ($LEB = Q_1 - 3H = -3200\,m^3\,s^{-1}\,km^{-1}$) and upper extreme boundary ($UEB = Q_3 + 3 \cdot H = 3022\,m^3\,s^{-1}\,km^{-1}$) were rejected before analysis of the time series; Q_1 and Q_3 are the lower and upper quartile, and H is the interquartile range. They represented ~3% of the whole time series. These pre-treated time series of $-Q_X$ were used to estimate upwelling rates of ENACW on the NW Iberian shelf at seasonal and fortnight time-scales.

Daily values of $-Q_X$ calculated from geostrophic winds in the $2^\circ \times 2^\circ$ cell centred at 43°N 11°W were compared with those calculated from winds measured at the 'Cape Finisterre' meteorological observatory from April to December 1997 (data not shown). They are well correlated ($r = +0.81$, $n = 275$), with a slope very close to 1 (0.92 ± 0.04). It demonstrates that the time series of $-Q_X$ used in this work is representative for the actual winds in the NW Iberian margin, both in terms of intensity and variability (M. Gilcoto, Unpub. data).

2.3. Time series of bottom shelf temperatures

A station in the 'Ría de Vigo' (grey point in Fig. 1) was visited twice a week from January 1987 to December 1999 and offers a useful time-series reference. The central and outer 'Ría de Vigo' behaves as an extension of the shelf, and it is under the direct influence of shelf winds (Blanton et al., 1987; Nogueira et al., 1997a, b). Gilcoto et al. (2001) combined wind and current meter data to demonstrate the dependence on shelf wind-stress of water circulation in the ría. These authors also observed that bottom (40 m) temperature at the time-series station responds to shelf winds with a delay of ~3 days; this is the time interval that ENACW needs to cover the 45 km from the 200 m isobath to the time-series station at an average speed of $\sim 0.2\,\mathrm{cm\,s^{-1}}$. Slight thermohaline modification of ENACW occurs during its transit across the shelf, resulting in an average net warming of +0.5°C at the time-series station compared with the temperature of ENACW at the 200 m isobath. Since we are working at the fortnight time-scale, the response of the water column to shelf winds is assumed to be instantaneous. The 1987–1999 time series of bottom temperatures ($n = 1352$) was used in this study to infer the thermohaline characteristics of upwelled ENACW between 42° and 43°N.

2.4. Statistical analysis of the meteorological and hydrographic data

Following Doval et al. (1997), the best fit between any pair of dependent (Y) and independent (X) variables can be obtained by minimising the following residuals function:

$$\sum_i [(X_i - \hat{X}_i)^{w_X} (Y_i - \hat{Y}_i)^{w_Y}]^2, \tag{2}$$

where w_X and w_Y are weights for the independent and dependent variables, respectively, with w_X, $w_Y \geqslant 0$ and $w_X + w_Y = 1$. The weighting factors are functions of the estimated experimental error (er) compared with the standard deviation (SD) of the whole set of measurements of the measured variables. For any pair of variables

$$w_X = \left(\frac{\mathrm{er}_X}{\mathrm{SD}_X}\right) \Big/ \left(\frac{\mathrm{er}_X}{\mathrm{SD}_X} + \frac{\mathrm{er}_Y}{\mathrm{SD}_Y}\right). \tag{3}$$

In order to simplify the linear regression analyses, all possible cases were condensed to two categories or models: (I) $w_X = 0, w_Y = 1$ and (II) $w_X = w_Y = 0.5$ (Sokal and Rolf, 1995). Model I was used when X was temperature and Y was salinity or a chemical variable. In these cases, $w_Y \gg w_X$. Model II was used when both X and Y were chemical variables and $w_Y \sim w_X$. Differences between models I and II increase as the correlation coefficient (r) decreases.

In addition, harmonic analysis (Poularikas and Seely, 1991) was applied to characterise the seasonal modes of temporal variability of $-Q_X$ at 43°N 11°W and bottom temperatures at the time-series station of the 'Ría de Vigo', and Box–Jenkins transfer-function models (Box and Jenkins, 1976) were used to predict the latter from the former variable at the fortnight time-scale.

2.5. Estimation of satellite-derived net community primary production rates

SeaWiFS-derived primary production rates were calculated for shelf waters (water depth <200 m) of the study area (42–43°N) following Joint et al. (2002). These authors used the semi-analytic model of Morel (1991) and Morel et al. (1996) to calculate daily primary production from January 1998 to December 1999. The model takes as input daily satellite-derived chlorophyll concentration, satellite sea-surface temperature, and downwelling irradiance at the sea-surface calculated from meteorological data and model

output. It is assumed that chlorophyll is constant with depth and equal to the surface (SeaWiFS measured) value. When no chlorophyll data could be derived for a particular day from SeaWiFS, primary production was calculated with chlorophyll values from the previous non-zero day but with the meteorological data for that day.

Morel et al. (1996) showed that the model produced values in close agreement with 24 h in situ incubations. Primary production estimated from 24 h incubations represents something close to the balance of the autotrophic production minus the respiration of the whole community of autotrophs and heterotrophs collected in the incubation bottle (mainly microzooplankton and bacteria) over the incubation time (Laws, 1991; Williams, 1993). Therefore, in the context of this work, satellite-derived primary production represents net microbial community production (NCP) rather than GPP. We have preferred to use the term NCP, commonly used for the dissolved oxygen method, rather than the term Net Primary Production (NPP), commonly used with the ^{14}C technique, because NPP only considers the respiration of autotrophs, according to the definitions of Williams (1993). In this sense, it has been observed in the NW Iberian margin during the upwelling season that PP estimated from 24 h ^{14}C incubations represent $\frac{1}{2}$ of PP estimated from 2 h ^{14}C incubations (Barbosa et al., 2001). Therefore, since respiration represents 50% of GPP, it is adequate to consider that PP estimates from 24 h ^{14}C incubations includes microheterotrophic (bacteria, flagellates, ciliates) respiration.

3. Results

3.1. Thermohaline and chemical characterisation of the ENACW off NW Spain

The potential temperature–salinity ($\theta-S$) plot of the 706 ENACW samples selected from the 128 stations occupied (Fig. 1) during the 14 hydrographic surveys off NW Spain (Table 1) is presented in Fig. 2a. Fiúza's (1984) ENACW reference line is also incorporated for comparison. Scattering around the reference line results from the inherent variability of the thermohaline characteristics of the source mode waters that produce the ENACW, which are strongly affected by the inter-annual variability of the NE Atlantic weather. Pérez et al. (1995) demonstrated a clear relationship between the thermohaline properties of the subtropical branch of ENACW ($\theta > 13^{\circ}C$ or $\sigma_0 < 27.1\,kg\,m^{-3}$) at 42°N and the decadal changes observed in the wind regime at the 43°N 11°W geostrophic cell. In any case, the effect of ENACW modes mixing on the nutrient variability can be adequately studied by linear regression with either salinity or temperature, because of the high correlation between the thermohaline properties ($r = +0.93$; Table 2). Temperature is preferred because the er/SD ratio (see Section 2.4) is 4.2×10^{-2} ($=0.005/0.12$) for salinity and only 5.3×10^{-3} ($=0.005/0.91$) for temperature.

Nitrate is strongly correlated with temperature in the ENACW domain ($r = -0.93$), in such a way that the standard error of the estimation of nitrate is $\pm 1.2\,\mu mol\,kg^{-1}$ (Table 2). Nitrate becomes zero for ENACW modes warmer than $14.8 \pm 0.4^{\circ}C$. It is also remarkable that the observed scatter around the regression line (Fig. 2b) is not related to the dispersion observed in the thermohaline properties (Fig. 2a). The residuals of the $S-\theta$ regression (ΔS) are not significantly correlated with the residuals of the NO_3–θ regression (ΔNO_3): $r = 0.01, p > 0.72$. In addition, the NO_3 residuals do not show a clear seasonal trend: they are slightly, but not significantly, higher during the winter cruises (data not shown). Phosphate is also strongly correlated with temperature ($r = -0.92$; Table 2). On the other hand, the silicate–temperature relationship (not shown) is described better with a parabolic rather than a linear function of θ ($r = -0.92$; Table 2), which indicates that the SiO_4–θ slope increases with decreasing temperature.

The direct nitrate–phosphate correlation is extremely high ($r = +0.97$; Table 2), as expected. The N/P slope of the correlation is 17.9 ± 0.2 mol $N\,mol\,P^{-1}$, about 12% higher than the Redfield value of 16 mol $N\,mol\,P^{-1}$ (Anderson, 1995), and an excess of $0.018 \pm 0.005\,\mu mol\,kg^{-1}$ of phosphate occurs at zero nitrate concentrations (Fig. 2c). The

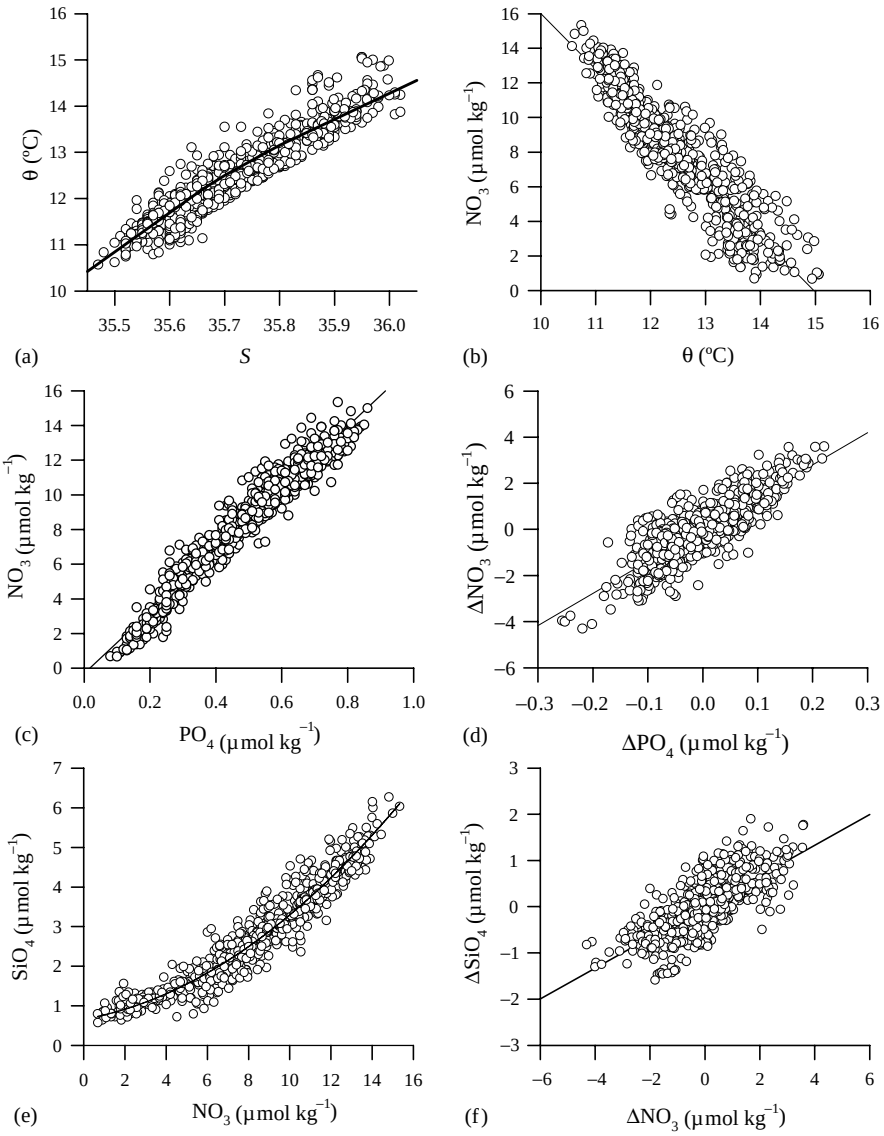

Fig. 2. $X-Y$ plots of the thermohaline and chemical properties of the ENACW upwelled off NW Spain. (a) Potential temperature versus salinity, (b) nitrate versus potential temperature, (c) nitrate versus phosphate, (d) nitrate versus phosphate anomaly, (e) silicate versus nitrate, and (f) silicate versus nitrate anomaly. Fiúza's (1984) ENACW reference line is included in panel (a) and regression lines (Table 2) in panels (b–f).

residuals of the NO_3–θ regression (ΔNO_3) are also strongly correlated with the residuals of the PO_4–θ regression (ΔPO_4) (Fig. 2d), with $r = +0.80$ and a Redfield N/P slope of 16.4 ± 0.5 mol N mol P^{-1}. The silicate–nitrate plot (Fig. 2e) shows the expected parabolic dependence ($r = +0.96$; Table 2) previously observed with temperature. It is also remarkable that there is an excess of $0.63 \pm 0.06\,\mu mol\,kg^{-1}$ of SiO_4 at zero NO_3. Finally, the residuals of the SiO_4–θ regression (ΔSiO_4) are also reasonably correlated with the residuals of the NO_3–θ regression (ΔNO_3): $r = +0.73$ (Fig. 2f; Table 2), with a Si/N slope of 0.48 ± 0.02 mol Si mol N^{-1}.

Table 2
Results of the linear regression analysis of nutrients (NO_3, PO_4, SiO_4) and thermohaline properties (S, θ) for all the ENACW samples at the oceanic stations (water depth >1000) off NW Spain between 42° and 43°N

Linear equation	r	n
$S(0.044) = 35.785(0.003) + 0.132(0.002)[\theta - 13^{\circ}C]$	+0.93	706
$NO_3(1.2) = 50.6(0.6) - 3.43(0.05)\theta$	−0.93	692
$PO_4(0.07) = 2.73(0.04) - 0.182(0.003)\theta$	−0.92	685
$SiO_4(0.5) = 65(3) - [8.8(0.5) - 0.30(0.02)\theta]\theta$	−0.92	615
$NO_3(0.8) = -0.34(0.09) + 17.9(0.2)\ PO_4$	+0.97	685
$\Delta NO_3\ (0.7) = 16.4(0.5)\Delta PO_4$	+0.80	685
$SiO_4(0.3) = 0.63(0.06) + [0.10(0.02) + 0.017(0.001)NO_3]NO_3$	+0.96	609
$\Delta SiO_4(0.4) = 0.48(0.02)\Delta NO_3$	+0.73	609

Note: The standard error of the estimation and the standard error of the regression coefficients are included in the regression equations. ΔNO_3,ΔPO_4, and ΔSiO_4, nitrate, phosphate and silicate residuals of the correlation with θ; r, correlation coefficient; n, number of observations.

3.2. Coupling between bottom shelf temperature and coastal winds off NW Spain

Fig. 3a shows the inter-annual variability of the fortnight-average $-Q_X$ time series from 1982 to 1999. Shaded areas ($-Q_X > 0$) define the duration and intensity of the upwelling season off NW Spain. Whereas the onset of the upwelling season is quite variable, ranging from mid-February to mid-May, the end of upwelling usually occurs in September or October. It is also noteworthy that downwelling-favourable periods may occur in the upwelling season, and vice versa. The box-and-whisker plot of Fig. 3b gives a better indication of the extreme inter-annual variability of the fortnight-average values of $-Q_X$ in the period 1987–1999. The average annual cycle of $-Q_X$, obtained from the first ($T = 24$ fortnights) and second ($T = 12$ fortnights) harmonics of a Fourier analysis, explains 37% of the total variability of the fortnight-average time-series of $-Q_X$. Considering this average annual cycle, the upwelling season extends from late March (5th fortnight) to late September (19th fortnight). Late May (10th fortnight) is usually a period of downwelling within the upwelling season.

The average 1987–1999 seasonal evolution of bottom temperature at the time-series station of the 'Ría de Vigo' (solid line in Fig. 3c) follows $-Q_X$, with minimum temperatures during the upwelling season and maximum during the downwelling season. Uplift of cold ENACW from 150–200 m depth produces the low bottom temperatures recorded during the spring and summer (Álvarez-Salgado et al., 1993), whereas horizontal advection of warm subtropical surface water results in high temperatures during the autumn and winter (Pingree, 1993). As expected, the downwelling-favourable period of late May (10th fortnight) is accompanied by a slight increase of bottom temperatures. The average annual cycle explains 40% of the total variability of the fortnight-average time-series of bottom temperature. As much as 70% of the fortnight-average bottom temperatures are in the 12–14°C range, with 13.0–13.5°C the most frequent values, which are observed 25% of the time in the period 1987–1999.

Average-fortnight bottom temperatures at the time-series station can be reasonably predicted from $-Q_X$ ($r = -0.78$, $p < 0.01$) and a Box–Jenkins transfer-function model that includes the seasonal cycles of both variables

$$\begin{aligned}\theta(t) = \mathrm{SC}\{\theta\} &+ [4.2(\pm 1.1)\,(Q_X(t) - \mathrm{SC}\{Q_X(t)\}) \\ &+ 6.9(\pm 1.1)\,(Q_X(t-1) - \mathrm{SC}\{Q_X(t-1)\}) \\ &+ 5.0(\pm 1.1)\,(Q_X(t-2) - \mathrm{SC}\{Q_X(t-2)\}) \\ &+ 3.9(\pm 1.1)\,(Q_X(t-3) \\ &- \mathrm{SC}\{Q_X(t-3)\})]\,10^{-4}, \end{aligned} \quad (4)$$

where $\theta(t)$ is the predicted average bottom temperature at the time-series station during the fortnight 't'. $\mathrm{SC}\{\theta\}$ is the seasonal cycle (first and second harmonics of the Fourier analysis of the

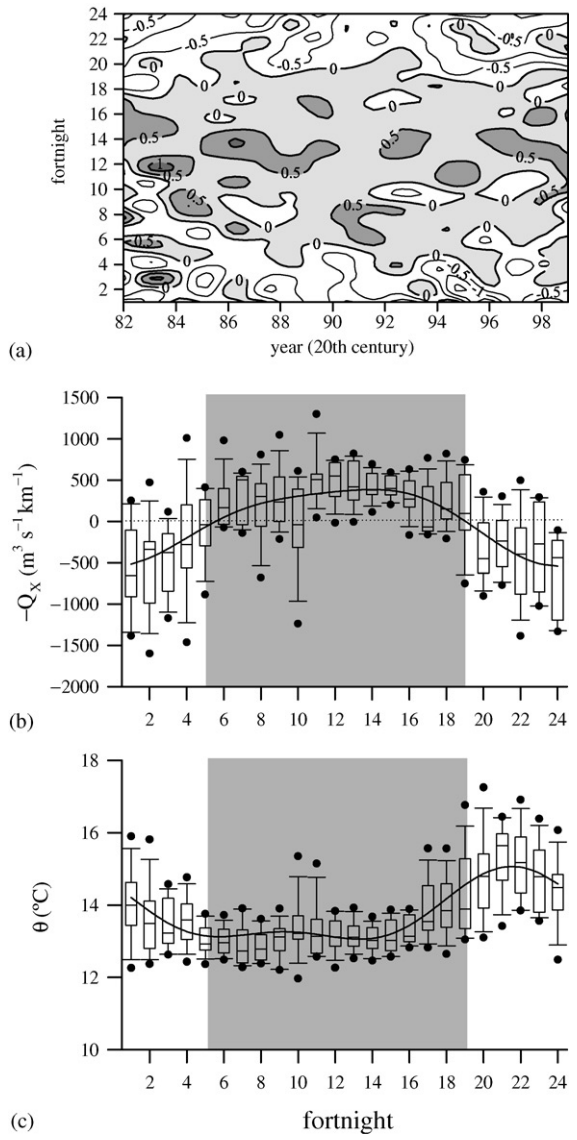

Fig. 3. (a) Inter-annual variability of the fortnight-average time-series of the offshore Ekman transport at 43°N 11°W ($-Q_X$) from 1982 to 1999. Box-and-whisker plots of the fortnight-average time-series of (b) $-Q_X$ and (c) bottom temperature at the time-series station of the 'Ría de Vigo' from 1987 to 1999. Fifty per cent of the data are included within the limit of the boxes, the caps represent the 10th and 90th percentiles and the solid lines within the boxes represents the median. The black dots are observations out of the 10th and 90th percentiles. The solid curves in panels (b) and (c) are the average 1987–1999 seasonal cycles of $-Q_X$ and bottom temperature obtained from the harmonics of a Fourier analysis. Grey shaded areas in panel (a) represents $-Q_X > 0$ and in panels (b) and (c) represents the upwelling season.

1987–1999 time series) of bottom temperature. $Q_X(t)$, $Q_X(t-1)$, $Q_X(t-2)$ and $Q_X(t-3)$ are the recorded fortnight-average values of Q_X during the fortnights 't', '$t-1$', '$t-2$' and '$t-3$', respectively. Finally, $SC\{Q_X(t)\}$, $SC\{Q_X(t-1)\}$, $SC\{Q_X(t-2)\}$ and $SC\{Q_X(t-3)\}$ are the seasonal cycles of Q_X. It is remarkable that, once the seasonal cycles have been removed, bottom temperatures are more affected by wind-stress values in the previous (coefficient 6.9 ± 1.1) than in the current (coefficient 4.2 ± 1.1) fortnight. Finally, Eq. (4) also indicates that higher $-Q_X$ values produce upwelling of colder (i.e. deeper) ENACW branches.

3.3. Estimation of new production on the NW Iberian shelf

Combination of (1) the 1987–1999 fortnight-average bottom temperatures at the time-series station, (2) the nitrate–temperature relationships in the ENACW domain, and (3) the 1987–1999 fortnight-average $-Q_X$ values at the 43°N 11°W geostrophic cell allows estimation of the fortnight-average NP in shelf waters of the NW Iberian shelf, from 42°N (River Miño) to 43°N Cape Finisterre (Fig. 1)

$$\mathrm{NP}(t) = -Q_X(t)\,\mathrm{NO_3}[\theta(t)]\,\frac{L}{A}, \tag{5}$$

where L is the distance between 42° and 43°N (110 km), i.e. the linear segment of coast where coastal upwelling occurs, and A is the surface area of the NW Iberian shelf (water depth <200 m) in this latitudinal range (3500 km^2). $NO_3[\theta(t)]$ is the NO_3 concentration calculated from the regression Eq. (2) (Table 2) with the bottom temperatures recorded at the time-series station, corrected by -0.5°C to take into account the average warming of upwelled ENACW during its transit across the shelf. NO_3 values are nil for temperatures >14.8°C. This nutrient has been chosen because it is probably the limiting element for the NW Iberian shelf, as suggested by the PO_4 and SiO_4 excess observed at NO_3 zero (Section 3.1). At the fortnight time-scale, total consumption of the upwelled NO_3 occurs in shelf euphotic waters, so nitrate flux calculated in Eq. (5) equals the

expected NP of the ecosystem. This calculation is also based on the assumption of bi-dimensionality of the upwelling processes on the NW Iberian margin, recently demonstrated by Álvarez-Salgado et al. (2000). NP has been set to zero for any $-Q_X<0$, i.e. when downwelling conditions occurs. This is a very reasonable assumption, because during a downwelling event, the NW Iberian shelf is occupied by warm ($>15°C$) nitrate-depleted surface ocean waters. The contribution of continental runoff to NP off NW Spain can be neglected: average continental runoff and offshore Ekman transport off the Rías Baixas is $30\,l\,s^{-1}\,km^{-2}$ of drainage basin and $270\,m^3\,s^{-1}\,km^{-1}$ of coast during the upwelling season (Nogueira et al., 1997a). Considering a total drainage basin of $\sim 6800\,km^2$ and a coast 110 km long, only 0.7% of surface waters on the shelf originates from land. Finally, NP rates calculated with Eq. (5) are in nitrogen units. A Redfield C/N molar ratio of 6.7 (Anderson, 1995) was used to convert them into carbon units. A recent paper by Pérez et al. (2000) demonstrates that, at the time scale of the upwelling season off NW Spain the ratio of inorganic carbon to nitrogen consumption is Redfield. The standard error of the estimation of NP rates (average relative error 30%) was based on a standard error of $\pm 1.2\,mmol\,m^{-3}$ for the estimation of nitrate from temperature (regression Eq. (2) in Table 2) and a relative error of 10% for the calculation of $-Q_X$. The results are not significantly different when observed or modelled (Eq. (4)) temperatures are used: the average difference between the two estimates is about half of the standard error of the estimation of NP.

Fig. 4a shows the box-and-whisker plot of the fortnight-average NP between the 5th and 19th fortnights from 1987 to 1999. The average seasonal cycle (solid line) is also shown, indicating minimal values ($<300\,mg\ C\,m^{-2}\,d^{-1}$) at the beginning and end of the upwelling season and maximal NP values ($>800\,mg\ C\,m^{-2}\,d^{-1}$) during July. As expected, a local minimum is observed at the 10th fortnight. However, the plot shows a very high inter-annual variability of fortnight-average NP. In fact, the seasonal cycle explains only 15% of the observed variability. NP, averaged over the upwelling season (5th–19th fortnights) from 1982 to 1999, indicate pronounced inter-annual variability (Fig. 4b), which accompanies the inter-annual variability of $-Q_X$ (Fig. 3a and b). NP for the periods 1982–1986 and 1996–1997 (open bars), when bottom temperatures are not available, was estimated from temperatures predicted by Eq. (4). Upwelling-season average NP ranges from 330 to $815\,mg\ C\,m^{-2}\,d^{-1}$ ($75–200\,g\ C\,m^{-2}\,(7.5\ month)^{-1}$), with a 1982–1999 average of $490\pm145\,mg\,C\,m^{-2}\,d^{-1}$ or $110\pm30\,g\,C\,m^{-2}\,(7.5\ month)^{-1}$.

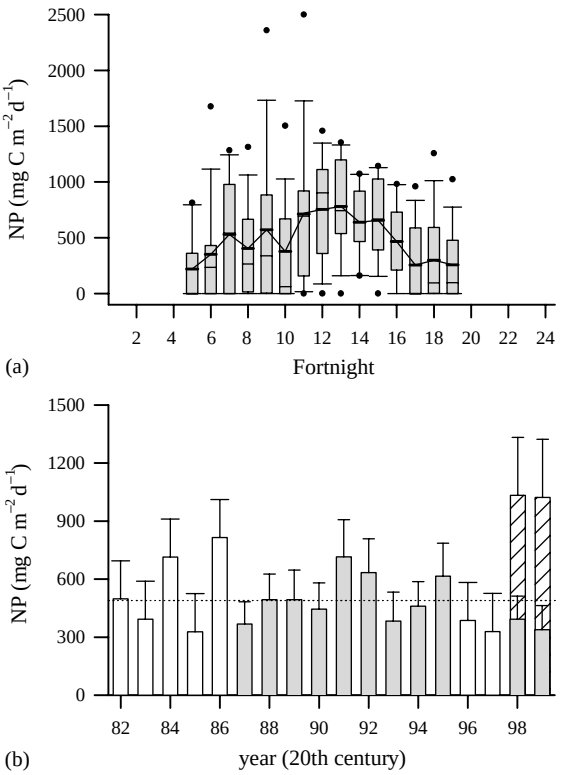

Fig. 4. (a) box-and-whisker plots of the fortnight-average 1987–1999 time-series of NP rates in shelf waters off NW Spain (42°–43°N) calculated with Eq. (5). Fifty per cent of the data are included within the limit of the boxes, the caps represent the 10th and 90th percentiles and the solid line in the box represents the median, the solid is the average 1987–1999 NP and the black dots are the values out of the 10th and 90th percentiles. (b) Inter-annual variability of the average over the upwelling season NP from 1982 to 1999. Open bars were calculated with Eq. (6) and grey bars with Eq. (5). The hatched bars represent satellite-derived NCP rates for 1998 and 1999. The dotted line is the average NP from 1982 to 1999.

Fig. 4b also compares the satellite-derived NCP (coarse bars) and the NP (grey bars) for the upwelling seasons of years 1998 and 1999, when SeaWiFS images are available. The upwelling-season average NP/NCP ratio is 0.35 for 1998 and 0.30 for 1990, indicating that about 65–70% of the net community primary production is respired over the NW Iberian shelf.

4. Discussion

4.1. Nutrient ratios in upwelled ENACW—implications for NP of the NW Iberian upwelling

Nutrient levels of ENACW upwelled off NW Spain are remarkably low compared with central waters of the other major coastal upwelling systems of the world ocean. NO_3 on the Iberian margin ranges from $2.6 \pm 1.3\,\mu mol\,kg^{-1}$ for subtropical ENACW of 14°C to $9.4 \pm 1.2\,\mu mol\,kg^{-1}$ for subpolar ENACW of 12°C. For comparison, the aged South Atlantic Central Water (SACW) that upwells off Cape Blanc (NW Africa) or SW Africa has about $20\,\mu mol\,kg^{-1}$ NO_3 and Pacific central waters off California and Peru transport from 10 to $30\,\mu mol\,kg^{-1}$ NO_3 (see review by Castro et al., 2000). According to Eq. (5), these low nutrient levels have a direct effect on the NP rates of the NW Iberian margin. Since wind regimes (intensity, persistence) in the four major upwelling systems of the World Ocean are similar when comparable latitudes (>40°N or S) are considered (Bakun and Nelson, 1991), the NP of NW Spain would be less than half than off Oregon or Chile.

The dependence of NO_3 and PO_4 levels on the mixing of subtropical and subpolar ENACW branches is partly responsible for the covariance between these two nutrients. The linear regression with temperature and the subsequent revision of the correlation between the residuals of the nutrient–temperature relationships allow the separation of the effects of mixing and biogeochemistry from the nutrient signals. Linear regressions with temperature suggest that the N/P ratio of subpolar nutrient-rich ENACW of 12°C is 17.3 mol N mol P^{-1}, and of subtropical nutrient-poor ENACW of 14°C is 14.2 mol N mol P^{-1}. Therefore, the relatively high N/P slope of the linear regression between NO_3 and PO_4 is partly due to the mixing of ENACW branches with very different N/P ratios. In fact, the N/P slope obtained from nutrient concentrations of the 12°C and 14°C ENACW would be as high as 18.8 mol N mol P^{-1}. It should be noted that N/P ratios derived from the nutrient–temperature relationships retain not only the differences in the source regions but also the average 'large scale' mineralisation from the source regions to the study area. Therefore, it seems either that the organic materials exported from the photic layer of the subtropical and subpolar Eastern North Atlantic have a different composition or that phosphorus is mineralised relatively to nitrogen in the subtropical than in the subpolar ENACW. The subpolar North Atlantic is an area where a massive spring bloom of large diatoms occurs, whereas the subtropical North Atlantic is characterised by brief blooms dominated by flagellates (Longhurst, 1995). An important downward flux of biogenic materials is expected in the subpolar domain, whereas reduced export should occur in the subtropical domain (Legendre, 1998). On the other hand, ΔNO_3 and ΔPO_4, which are independent of the mixing of ENACW branches, keep a ratio of 16 mol N mol $^{-1}$ P. This indicates that 'local' mineralisation occurs with the expected Redfield value. It should be highlighted again that ΔNO_3 is not correlated with ΔS but with ΔPO_4, suggesting that the scatter observed in the nutrient–temperature relationships is essentially due to 'local' biogeochemical processes and that the decadal variability of ENACW source types has no significant effect.

The different composition of microplankton populations in subpolar and subtropical North Atlantic provinces could also be a reason for the parabolic SiO_4/NO_3 relationship. The N/Si ratio of subpolar waters of 12°C and subtropical waters of 14°C obtained from the regressions with temperature are 3.6 and 4.3 mol N mol^{-1} Si, respectively. ΔSiO_4, as for the case of ΔPO_4, also correlates with ΔNO_3, with a water-mass-mixing independent N/Si slope of 2.1 mol N mol^{-1} Si. The world average N/Si ratio of marine diatoms is

1 mol N mol^{-1} Si, although it is quite variable (Brzezinski, 1985). Assuming that the ratio for eastern North Atlantic diatoms is 1, the $\Delta NO_3/\Delta SiO_4$ slope observed off NW Spain suggests that (1) half of the phytogenic materials mineralised in the ENACW domain comes from diatoms or (2) only a part of the biogenic silica is mineralised at these shallow levels (Broecker and Peng, 1982; Dugdale et al., 1995).

Finally, the observed excess of PO_4 and SiO_4 at NO_3 concentrations of zero suggests that nitrogen is the limiting nutrient of primary production on the NW Iberian margin during the upwelling season. However, the SiO_4 excess of 0.63 ± 0.06 μmol kg^{-1} is within the wide range of threshold silicate concentrations necessary for diatom growth (0.3–2.0 μmol kg^{-1}; Paasche, 1973; Egge and Askens, 1992) and could also limit their development, as recently observed in other upwelling systems (Dugdale et al., 1995).

4.2. Dependence of NP on upwelling rates and the quality of upwelled water

Upwelling rates ($-Q_X$) control NP on the NW Iberian margin for two reasons: (i) because they dictate the flux of NO_3-rich ENACW (Eq. (5)) and (ii) because they set up the temperature (i.e. the NO_3 level) of the upwelled ENACW (Eq. (4)). With these considerations in mind, we have obtained the following regression equation ($r = +0.91$, $n = 144$) to estimate the NP obtained with Eq. (5) (in mg C m^{-2} d^{-1}) only from the time series of $-Q_X$

$$NP(\pm 197) = -[1.1(\pm 0.1) + 5(\pm 1)\,10^{-4}\,Q_X(t)] \times Q_X(t) - 0.15(\pm 0.04)\,Q_X(t-1). \quad (6)$$

As expected, it is a quadratic function of $-Q_X(t)$. In addition, there is a marked influence of the average upwelling rate during the previous fortnight, in agreement with the dependence of bottom temperatures on $-Q_X(t-1)$ (Eq. (4)). On the other hand, inclusion of the terms $-Q_X(t-2)$ and $-Q_X(t-3)$, which also appear in Eq. (4), do not significantly improve the estimation of NP with Eq. (6). Analysis of the regression coefficients of Eq. (6) indicates that $-Q_X(t)$ has a primary effect on the estimated NP, >7 times greater than $-Q_X(t-1)$. The effect of the quadratic coefficient ($5 \pm 1 \times 10^{-4}$), which enhances NP by 45 mg C m^{-2} d^{-1} for the upwelling-season average $-Q_X(t)$ of 270 m^3 s^{-1} km^{-1}, reflects the influence of coastal upwelling intensity on the quality (θ, NO_3 levels) of the upwelled water. During the intense upwelling events of the mid-summer, when $-Q_X(t)$ usually exceeds 500 m^3 s^{-1} km^{-1}, the quality of the upwelled water limits the enhancement of NP by greater than 25%.

This formula allows the prediction of NP rates in the NW Iberian upwelling from a simple times-series of coastal winds. The work of Blanton et al. (1987), who found a remarkably high correlation ($r = +0.80$) between the meat content of mussels collected in the 'Rías Baixas' and the offshore Ekman transport, emphasises the importance of Eq. (6) both from the viewpoint of the exploitation of resources and from the role of coastal upwelling systems in the regulation of the anthropogenic CO_2 excess accumulated in the atmosphere.

4.3. Fate of primary production in the NW Iberian upwelling

The community of heterotrophs not accounted for by the 24 h incubations (zooplankton, microheterotrophs of the aphotic layer, and benthic organisms) should be responsible for the calculated respiration of 65–70% of the NCP at the time scale of the upwelling season. Data on nutrient regeneration rates by zooplankton in the Iberian margin are scarce and relate to two short periods in May 1997 and September 1998 off the 'Ría de Vigo'. An average value of 15 mg N m^{-2} d^{-1} or 85 mg C m^{-2} d^{-1} (using a C/N molar ratio of 6.7) can be suggested from that set of measurements (Alcaraz, Pers. Comm.), which represents <10% of NCP. Therefore, most of the respiration of NCP occurs in the aphotic layer and the sediments. This result is in agreement with the extensive nutrient enrichment observed by Álvarez-Salgado et al. (1997) in shelf bottom waters, which represent from 25% (in May) to 50% (in September) of the expected NO_3 concentration of upwelled ENACW off the 'Rías Baixas'. This nutrient enrichment is the reason for the

higher area-specific NP rates usually observed in the 'Rías Baixas'. Upwelling-season average NP of 840 mg $C\,m^{-2}\,d^{-1}$ in the 'Ría de Arousa' during 1989 (Rosón et al., 1999) and 790 mg $C\,m^{-2}\,d^{-1}$ in the 'Ría de Vigo' during 1997 (Gago et al., 2002) were estimated with a box-model inverse method. For comparison, the upwelling-season average NP of the NW Iberian shelf was 495 ± 150 mg $C\,m^{-2}\,d^{-1}$ in 1989 and only 330 ± 195 mg $C\,m^{-2}\,d^{-1}$ during 1997. Outwelling of fresh phytogenic materials from the 'Rías Baixas' and subsequent sedimentation on the shelf seems to constitute the main substrate entry for the micropheterotrophs of the aphotic layer and the benthic communities on the shelf (Tenore et al., 1982, 1984; López-Jamar et al., 1992). In this sense, the intricate topography of the NW Iberian shelf favours the retention of primary production on the shelf. The average width of the shelf + rías system is about 50 km, whereas the extension of the Oregon and Peru shelves are 30 and 20 km, respectively (Smith, 1981).

Álvarez-Salgado et al. (2001) have estimated that 100 g $C\,m^{-2}$ are exported from the NW Iberian shelf to the surrounding oligotrophic ocean by the upwelling filament recurrently observed off the 'Ría de Vigo' during the upwelling season (Haynes et al., 1993). This number is very close to our 1982–1999 NP estimate of 110 ± 30 g $C\,m^{-2}$, suggesting that at the time scale of the upwelling season NP serves as a source of fresh phytogenic materials to the surrounding oceanic communities. In this sense, although coastal upwelling off NW Spain can be appropriately modelled with a 2-D approach (Álvarez-Salgado et al., 2000), off-shelf export mediated through upwelling filaments is clearly a 3-D process. Our upwelling-season average NP (490 ± 145 mg $C\,m^{-2}\,d^{-1}$) is $\sim$50% higher than the annual average world coastal zone NP of 315 mg $C\,m^{-2}\,d^{-1}$ (Wollast, 1998). However, if a NP close to zero is assumed during the 4.5 month downwelling-favourable period, then the estimated annual average NP of NW Iberian shelf waters would be 305 mg $C\,m^{-2}\,d^{-1}$, i.e. the same as the world coastal zone average. Since the Iberian margin is a coastal upwelling system, higher rates would be expected. The reasons behind the relatively low NP off NW Spain are (1) the seasonality of coastal upwelling, which operates only $\frac{2}{3}$ of the year at our latitudes, (2) The relatively low nutrient levels of upwelled ENACW (Section 4.1), and (3) the reduced continental inputs during the upwelling season—only 0.7% of surface waters on the shelf coming from the adjacent land mass.

Finally, Moncoiffé et al. (2000) demonstrated from 24 h in situ O_2 incubations at the time-series station of the 'Ría de Vigo' during the 1991 upwelling season that respiration in the photic layer represents about 40% of GPP. If we consider that this number is valid for NW Iberian shelf waters, the NCP/GPP ratio would be 0.60. Consequently, only $0.20 = (NP/NCP)(NCP/GPP) = 0.33 \times 0.60$ of GPP would be available to be exported out of the study system. It should be highlighted that this *f*-ratio is valid at the ecosystem-level (3500 km^2) and for an upwelling-season average ($7\frac{1}{2}$ month). It cannot be directly compared with the *f*-ratio obtained from ^{15}N incubations, which are only representative of the microplankton community (Wollast, 1998) at the spatial-scale of a few kilometres around the sampling site and the time scale of the incubation time (normally <24 h).

Acknowledgements

The authors wish to thank the crew and scientific parties who participated in the fourteen cruises referred in Table 1 for assistance and collaboration. Financial support for this work came from EU contracts MAS3-CT97-0076 (OMEX II-II), MAS2-CT93-0065 ('MORENA') and MAS1-CT90-0017 ('The Control of Phytoplankton Dominance').

References

Álvarez-Salgado, X.A., Rosón, G., Pérez, F.F., Pazos, Y., 1993. Hydrographic variability off the Rías Baixas (NW Spain) during the upwelling season. Journal of Geophysical Research 98, 14447–14455.

Álvarez-Salgado, X.A., Castro, C.G., Pérez, F.F., Fraga, F., 1997. Nutrient mineralization patterns in shelf waters of the

Western Iberian upwelling. Continental Shelf Research 17, 1247–1270.

Álvarez-Salgado, X.A., Gago, J., Míguez, B.M., Gilcoto, M., 2000. Surface waters of the NW Iberian margin: upwelling on the shelf versus outwelling of upwelled waters from the Rías Baixas. Estuarine, Coastal and Shelf Science 51, 821–837.

Álvarez-Salgado, X.A., Doval, M.D., Borges, A.V., Joint, I., Frankignoulle, M., Woodward, E.M.S., Figueiras, F.G., 2001. Off-shelf fluxes of labile materials by an upwelling filament in the NW Iberian upwelling system. Progress in Oceanography 51, 321–337.

Anderson, L.A., 1995. On the hydrogen and oxygen content of marine phytoplankton. Deep-Sea Research I 42, 1675–1680.

Bakun, A., 1973. Coastal upwelling indices, west coast of North America, 1946–71. NOAA Technical Report NMFS-671, 103pp.

Bakun, A., Nelson, C.S., 1991. The seasonal cycle of wind-stress curl in subtropical eastern boundary current regions. Journal of Physical Oceanography 21, 1815–1834.

Barbosa, A.B., Galvão, H.D., Mendes, P., Álvarez-Salgado, X.A., Figueiras, F.G., Joint, I., 2001. Short-term variability of heterotrophic bacterioplankton during upwelling off the NW Iberian margin. Progress in Oceanography 51, 339–359.

Blanton, J.O., Tenore, K.R., Castillejo, F.F., Atkinson, L.P., Schwing, F.B, Lavín, A., 1987. The relationship of upwelling to mussel production in the rías on the western coast of Spain. Journal of Marine Research 45, 497–511.

Box, G.E.P, Jenkins, G.M., 1976. Time series analysis, forecasting and control. Holden-Day, San Francisco, CA.

Behrenfeld, M.J., Falkowski, P.G., 1997. Phtotosynthetic rates derived from satellite-based chlorophyll concentration. Limnology and Oceanography 42, 1–20.

Broecker, W.S., Peng, T.K., 1982. Tracers in the Sea. Eldigio Press, New York, USA, 690pp.

Brzezinski, M.A., 1985. The Si:C:N ratio of marine diatoms: interspecific variability and the effect of some environmental variables. Journal of Phycology 21, 347–357.

Castro, C.G., Pérez, F.F., Álvarez-Salgado, X.A., Fraga, F., 2000. Coupling between thermohaline and chemical fields during two contrasting upwelling events off the NW Iberian Peninsula. Continental Shelf Research 20, 189–210.

Doval, M.D., Álvarez-Salgado, X.A., Pérez, F.F., 1997. Dissolved organic matter in a coastal embayment affected by upwelling. Marine Ecology Progress Series 157, 21–37.

Dugdale, R.C., Wilkerson, F.P., Minas, H.J., 1995. The role of a silicate pump driving new production. Deep-Sea Research I 42, 697–719.

Egge, J.K., Askens, D.L., 1992. Silicate as regulating nutrient in phytoplankton competition. Marine Ecology Progress Series 83, 281–289.

Eppley, R.W., Peterson, B.J., 1979. Particulate organic matter flux and planktonic new production in the deep ocean. Nature 282, 677–680.

Fiúza, A.F.G., 1984. Hidrología e Dinâmica das Aguas Costeiras de Portugal. Ph.D. Thesis, University of Lisbon, 294pp.

Gago, J., Álvarez-Salgado, X.A., Pérez, F.F., Gilcoto, M., 2002. Contrasting fate of dissolved and suspended organic carbon in a coastal upwelling system ('Ría de Vigo', NW Iberian Peninsula). Estuarine, Coastal and Shelf Science, in press.

Gilcoto, M., Álvarez-Salgado, X.A., Pérez, F.F., 2001. Computing optimum estuarine residual fluxes with a multi-parameter inverse method (OERFIM). Application to the 'Ría de Vigo' (NW Spain). Journal of Geophysical Research 106, 13303–13318.

Haynes, R., Barton, E.D., Pilling, I., 1993. Development, persistence and variability of upwelling filaments off the Atlantic Coast of the Iberian Peninsula. Journal of Geophysical Research 98, 22681–22692.

Hidy, G.M., 1972. A view of recent air–sea interaction research. Bulletin of the American Meteorological Society 53, 1083–1102.

Joint, I., Groom, S., Wollast, R., Chou, L., Tilstone, G.H., Figueiras, F.G., Loijens, M., Smyth, T.J., 2002. The response of phytoplankton production to periodic upwelling and relaxation events at the Iberian shelf break: estimates by the ^{14}C method and by satellite remote sensing. Journal of Marine Systems 32, 219–238.

Kauner, G.A., 1993. Productivity and new production of the oceanic system. In: Wollast, R., Mackenzie, F.T., Chou, L. (Eds.), Interactions of C, N, P and S. Biogeochemical cycles and global change. NATO ASI series, Vol. 14. Springer, Berlin, pp. 211–231.

Lavín, A., Díaz del Río, G., Cabanas, J.M., Casas, G., 1991. Afloramiento en el noroeste de la península Ibérica. Indices de afloramiento para el punto 43 grados N y 11 grados W periodo 1966–1989. Informes Técnicos del Instituto Español de Oceanografía, no. 91, 40pp.

Laws, E.A., 1991. Photosynthetic quotients, new production and net community production in the open ocean. Deep-Sea Research I 38, 143–167.

Legendre, L., 1998. Flux of particulate organic material from the euphotic zone of oceans: estimation from phytoplankton biomass. Journal of Geophysical Research 103, 2897–2903.

Longhurst, A., 1995. Seasonal cycles of pelagic production and consumption. Progress in Oceanography 36, 77–166.

López-Jamar, E., Cal, R.M., González, G., Hanson, R.B., Rey, J., Santiago, G., Tenore, K.R., 1992. Upwelling and outwelling effects on the benthic regime of the continental shelf off Galicia, NW Spain. Journal of Marine Research 50, 465–488.

Moncoiffé, G., Álvarez-Salgado, X.A., Figueiras, F.G., Savidge, G., 2000. Seasonal and short-time-scale dynamics of microplankton community production and respiration in an inshore upwelling system. Marine Ecology Progress Series 196, 111–126.

Morel, A., 1991. Light and marine photosynthesis: a spectral model with geochemical and climatological implication. Progress in Oceanography 26, 263–306.

Morel, A., Antoine, D., Babin, M., Dandonneau, Y., 1996. Measured and modelled primary production in the north-east Atlantic (EUMELI JGOFS program): the impact of natural variations in photosynthetic parameters on model predictive skill. Deep-Sea Research I 43, 1273–1304.

Middleburg, J.J., Vlug, T., Van der Nat, F.J.W.A., 1993. Organic matter mineralization in marine systems. Global Planetary Change 8, 47–58.

Nogueira, E., Pérez, F.F., Ríos, A.F., 1997a. Seasonal patterns and long-term trends in an estuarine upwelling ecosystem (Ría de Vigo, NW Spain). Estuarine, Coastal and Shelf Science 44, 285–300.

Nogueira, E., Pérez, F.F., Ríos, A.F., 1997b. Modelling thermohaline properties in an estuarine upwelling ecosystem (Ria de Vigo, NW Spain) using Box–Jenkins transfer function models. Estuarine, Coastal and Shelf Science 44, 685–702.

Paasche, A., 1973. Silicon and the ecology of marine plankton diatoms. II. Silicate-uptake kinetics in five diatom species. Marine Biology 19, 262–269.

Pérez, F.F., Mouriño, C., Fraga, F., Ríos, A.F., 1993. Displacement of water masses and remineralization rates off the Iberian Peninsula by nutrient anomalies. Journal of Marine Research 51, 869–892.

Pérez, F.F., Ríos, A.F., King, B.A., Pollard, R.T., 1995. Decadal changes of θ–S relationship of the Eastern North Atlantic Central Water (ENAW). Deep-Sea Research I 42, 1849–1864.

Pérez, F.F., Álvarez-Salgado, X.A., Rosón, G., 2000. Stoichiometry of the net ecosystem metabolism in a coastal inlet affected by upwelling. The Ria de Arousa. NW Spain. Marine Chemistry 69, 217–236.

Pingree, R.D., 1993. Flow of surface waters to the west of the British Isles and in the Bay of Biscay. Deep-Sea Research II 40, 369–388.

Poularikas, A.D., Seely, S., 1991. Signals and Systems, 2nd Edition. PWS-KENT Publishing Company, Boston, 1015pp.

Quiñones, R.A., Platt, T., 1991. The relationship between the f-ratio and the P:R ratio in the pelagic ecosystem. Limnology and Oceanography 36, 211–213.

Ríos, A.F., Pérez, F.F., Fraga, F., 1992. Water masses in upper and middle North Atlantic Ocean east of the Azores. Deep-Sea Research I 39, 645–658.

Rosón, G., Álvarez-Salgado, X.A., Pérez, F.F., 1999. Carbon cycling in a large coastal embayment affected by wind driven upwelling: short-time-scale variability and seasonal differences. Marine Ecology Progress Series 176, 215–230.

Strickland, J.D.H., Parsons, T.R., 1972. A practical Handbook of Seawater Analysis, 2nd Edition. Bulletin of the Fisheries Research board, Canada, p. 167.

Smith, R.L., 1981. A comparison of the structure and variability of the flow field in three coastal upwelling regions: Oregon, Northwest Africa and Peru. In: Richards, F.A. (Ed.), Coastal Upwelling Series, Coastal and Estuarine Science, Vol. 1. AGU, Washington, pp. 107–118.

Sokal, R.R., Rolf, F.J., 1995. Biometry. Freeman and Company, New York, 887pp.

Tenore, K.R., Boyer, L.F., Cal, R.M., Corral, J., García-Fernández, C., González, N., González-Gurriaran, E., Hanson, R.B., Iglesias, J., Krom, M., López-Jamar, E., McClain, J., Pamatmat, M.M., Pérez, A., Rhoads, D.C., Santiago, G.D., Tietjen, J., Westrich, J., Windom, H.L., 1982. Coastal upwelling in the Rías Bajas, NW Spain: contrasting the Benthic regimes in the Rías of Arosa and Muros. Journal of Marine Research 40, 701–720.

Tenore, K.R., Cal, R.M., Hanson, R.B., López-Jamar, E., Santiago, G., Tietjen, J.H., 1984. Coastal upwelling off the Rías Bajas, Galicia, Northwest Spain. II: Benthic studies. Rapports et Procès-verbeaux des Rèunions, Conseil International pour l'Exploration de la mer 183, 91–100.

Wafar, M.V.M., Le Corre, P., l'Helguen, S., 1995. F-ratios calculated with and without urea uptake in nitrogen uptake by phytoplankton. Deep-Sea Research I 42, 1669–1674.

Walsh, J.J., 1991. Importance of continental margins in the marine biogeochemical cycling of carbon and nitrogen. Nature 359, 53–55.

Williams, P.J.le B., 1993. Chemical and tracer methods for measuring plankton production. ICES Marine Sciences Symposium 197, 20–36.

Wollast, R., 1993. Interactions of carbon and nitrogen cycles in the Coastal zone. In: Wollast, R., Mackenzie, F.T., Chou, L. (Eds.), Interactions of C, N, P and S. Biogeochemical cycles and global change. NATO ASI series, Vol. 14. Springer, Berlin, pp. 195–210.

Wollast, R., 1998. Evaluation and comparison of the global carbon cycle in the coastal zone and in the open ocean. In: Brink, K.H., Robinson, A.R. (Eds.), The Global Coastal Ocean. The Sea, Vol. 10. Wiley, New York, pp. 213–252.

Wooster, W.S., Bakun, A., Mclain, D.R., 1976. The seasonal upwelling cycle along the eastern boundary of the North Atlantic. Journal of Marine Research 34, 131–141.